ROYAL SOCIETY OPEN SCIENCE

royalsocietypublishing.org/journal/rsos

Research

Cite this article: Boeye AT, Atkins-Weltman KL, King JL, Swann S. 2026 Evidence of bird-like foot function in *Tyrannosaurus*. *R. Soc. Open Sci.* **13**: 252139.
https://doi.org/10.1098/rsos.252139

Received: 4 November 2025
Accepted: 16 December 2025

Subject Category:
Organismal and evolutionary biology

Subject Areas:
biomechanics, ecology, palaeontology

Keywords:
biomechanics, palaeontology, *Tyrannosaurus*

Author for correspondence:
Adrian Tussel Boeye
e-mail: aboeye26@coa.edu

Evidence of bird-like foot function in *Tyrannosaurus*

Adrian Tussel Boeye[1], Kyle Logan Atkins-Weltman[2], J. Logan King[3] and Scott Swann[†]

[1]College of the Atlantic, Bar Harbor, ME, USA
[2]Department of Anatomy and Cell Biology, Oklahoma State University College of Osteopathic Medicine, Tulsa, OK 81625, USA
[3]Colorado Northwestern Community College, Craig, CO 81625, USA

ATB, 0009-0006-3440-4427; KLA-W, 0009-0000-2914-6239; JLK, 0000-0003-2104-4187

The movement of extinct animals has been of long-standing interest, with *Tyrannosaurus rex* being a locus for this fascination. Foot-fall kinematics within *T. rex* and their effect on stride length (SL) and locomotion have yet to be investigated thoroughly, despite their impacts on the potential speed of *T. rex*. Here, we present novel findings on the function of the foot of *T. rex*, using three predictive allometry-based equations and several statistical tests including Kruskal–Wallis tests to reveal a complex and bird-like function of the foot. This includes a very bird-like gait defined by higher stride frequencies, proportionally short SLs and elevated speeds. Comparisons between the four sampled specimens of *T. rex* with extant bipedal species are more akin to the gaits of the ground-truth modelled *Struthio camelus* and are notably divergent from the modelled *Homo sapiens*. Additionally, our models are consistent with recent studies suggesting slower to more intermediate top speeds for adult *Tyrannosaurus* that fall within the range of 5–11 m s^{-1}. This study lays the groundwork for future studies to add comparisons with additional theropods and potentially identify ecological differences between species.

1. Introduction

Extant avian dinosaurs are one of the most successful and speciose tetrapod lineages, with over 10 000 species of birds formally recognized, ranging from diminutive hummingbirds to large palaeognaths [1]. However, crown birds are dwarfed in body size by many of their Mesozoic dinosaurian predecessors, whose masses could reach upwards of 20 000 000 times larger than the smallest known birds [2,3]. Given the immense size of many Mesozoic dinosaurs, this begets the question of how

[†]Deceased on April 16th, 2025.

Supplementary material is available online at https://doi.org/10.6084/m9.figshare.c.8262492.

THE ROYAL SOCIETY PUBLISHING

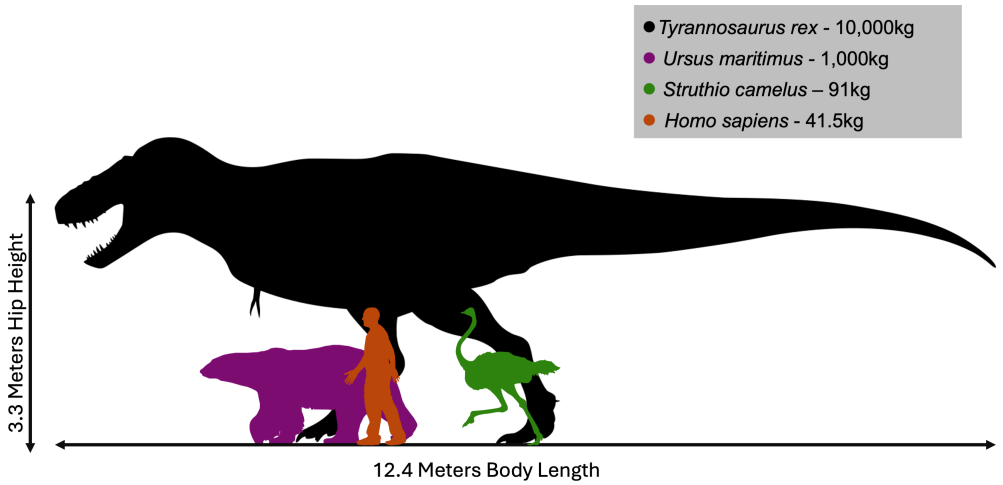

Figure 1. Size comparison between *T. rex* and several extant terrestrial vertebrates. Silhouettes are sourced from Phylopic (Phylopic.org). *Tyrannosaurus rex*, credit to Matt Dempsey; *Struthio camelus*, credit to Ferran Seyol; *Ursus maritimus*, Margot Michaud; *Homo sapiens*, Andrew Farke. Silhouettes are scaled relative to one another and recoloured for the purposes of comparison. Links to the original image repository are provided in the electronic supplementary material, S1.

they moved to successfully find and acquire food to support the metabolic needs associated with large body sizes, particularly for predators which need to track and capture their prey [4,5]. The need for food acquisition creates evolutionary pressure on giant predators to be fast enough to catch their prey and/or to successfully subdue and kill their prey [4–9].

The largest known dinosaurian predator was *Tyrannosaurus rex*, with the largest specimens potentially massing more than 10 tonnes [10], making it the largest terrestrial predator we have evidence for in the fossil record [11] (figure 1). By comparison, exceptionally large examples of *Ursus maritimus* reach 1000 kg [12], while other dinosaurian predators such as *Allosaurus* or *Gorgosaurus* could reach several tonnes with other taxa such as *Giganotosaurus* or *Acrocanthosaurus* tipping the scales at 8 tonnes [13,14]. Numerous well-preserved skeletons and decades of high-quality biomechanical research make *T. rex* the quintessential example of an exemplar taxon from which biomechanical data can be extracted [10,15]. Studies on locomotion are significant to trophic and ecological interpretations of *T. rex*, including the direct implications of its ecology and how *Tyrannosaurus* acquired food as a documented active predator [4,5,16].

Many studies have reconstructed the locomotion and estimated the maximum speed of a variety of extinct dinosaurs across different clades, including comparative [17–19] and more taxonomically restrictive analyses [7,20,21], but they have not considered the effects of foot-strike patterns, defined as which part of the foot strikes the ground first. Excluding foot-strike patterns in biomechanical calculations opens interesting questions on how they affect an animal's gait, since there is a wealth of anatomical data on the structure and function of the ankle and foot [22–26] and ichnological data from trackways [27,28]. Trackways attributed to tyrannosaurs suggest the pattern of force distribution is bird-like [28–30], with a 'distal-first' foot-strike pattern where flesh of the foot ventral to the distal pedal phalanges make initial contact with the ground as the animal moves [31–34]. The tracks of tyrannosaurs are tridactyl and, in limited cases, tetradactyl, caused by the hallux contacting the substrate [31,32,34,35]. Digits II and III are positioned in closer association to each other, whereas digit IV is typically displaced laterally relative to the other two digits [31,32,34,35]. In some well-preserved trackways of tyrannosaurs [34,36], digits III and IV appear to have a greater depth than impressions left by digit II, creating two distinct depressions in areas around the proximal pedal phalanges, with one centred on digits II and III and a second on digit IV [31,34–36].

Because several trackways from different localities and environments have been identified that maintain a consistent pattern of pedal digits interacting with the ground, these direct observations support the potential for bird-like locomotion in *T. rex*. The consequences for bird-like pedal locomotion among tyrannosaurs warrants further investigation through biomechanical modelling. Bird-like locomotion and bird-like running is defined in this study by the importance of ground contact time, proportionally short stride lengths (SLs) compared to standing hip heights, elevated stride frequencies compared to other animals of similar sizes, a smooth transition between walking and running gaits, moderately increased top speeds and low contact low contact forces with the ground when moving

[37,38]. To attain fast forward motion, bird-like running is a result of rapid changes in the position of the centre of mass of the body and the hindlimbs, while non-bird-like running is defined by a non-compliant, spring-like motion in the legs with running facilitated by elastic energy recovery as seen in humans [37].

In both birds and humans, these distinct locomotor strategies are products of their distinct postures, anatomy and positioning of the centre of mass. The digitigrade posture, sub-horizontal position of the femora, horizontal thoracic spinal column and anteriorly pitched whole body centre of mass facilitate more compliant limbs, increasing strain per unit stress [37,38]. This limb compliance enables greater stability both in locomotion and of the position of the head and cervical spine, as well as supporting the thoracic spinal column and anteriorly pitched centre of mass of the body. However, this compliant locomotion and resulting strain causes a reduction in elastic energy storage by virtue of hindlimb posture. By contrast, human posture is plantigrade, with a near-vertical position of the thoracic spinal column and centre of mass. This upright posture exchanges limb compliance and ground contact time for a style of locomotion defined by cyclical storage and release of elastic energy, resulting in a non-compliant, spring-like motion in the legs with low strain and reduced muscular effort [37]. Previous consensus anticipated notable differences in kinematics between the locomotion of theropod dinosaurs and modern birds on anatomical grounds centred on the presence of a muscular tail and hindlimb morphology [37,39], as such, bird-like running in *T. rex* in the context of bird-like pedal locomotion would represent a significant change in how the animal was understood to have moved.

In this study, we compiled a broad dataset of measurements on *Tyrannosaurus* specimens from the literature, which included data on hip height, dimensions of the hindlimb [40–43] and insight from the locomotion of extant avians [38,44]. Data are input into equations and then modified to be used by different animals across a broader variety of gaits [17,19,45]. We test the hypothesis that 'distal-first' strike patterns will increase stride frequency and thus change the potential top speed of an extinct animal [46] against the null hypothesis that changes in foot-strike patterns will have no effect on stride frequency and top speed estimates [46].

2. Material and methods

Institutional Abbreviations. BHI: Black Hills Institute, Hill City, SD, USA; BMR: Burpee Museum of Natural History, Rockford, IL, USA; MOR: Museum of the Rockies, Bozeman, MT, USA; NHMAD: Natural History Museum Abu Dhabi, Abu Dhabi, UAE; FMNH: Field Museum of Natural; History, Chicago, IL, USA; USNM: United States National Museum, Washington, DC, USA; LACM: Museum of Natural History Los Angeles, CA, USA.

Biomechanical Abbreviations. SL: stride length; RSL: relative stride length; DFS, distal-foot strike; MFS, mid-foot strike; RFS, rear-foot strike.

2.1. Specimens

We considered *T. rex* specimens MOR 555 (USNM 555000), FMNH PR 2081, the former BHI 3033 and LACM 23845 because of their (i) high skeletal completeness, (ii) data availability, and (iii) potentially distinct ontogenetic stages and/or size differences. This allows for results to be informative across body size and ontogenetically dependent niche differentiation [10,47–50]. We do note BMR P2002.4.1 which has previously been understood to be an immature *T. rex* [48,51], a body of comprehensive work shows this specimen belongs to the taxon *Nanotyrannus lethaeus* [52–56]. As such, while this specimen has been included in previous analyses studying the locomotion of *Tyrannosaurus* [10], we opt to use the specimen LACM 23845 which preserves a mostly complete hindlimb series, using BMR P.2002.4.1 as a point of comparison with measurements referenced in the electronic supplementary material, file S1. Ideally, this will allow future works to better resolve biomechanical implications across Tyrannosauroid phylogeny. BHI 3033 is no longer at its original repository [57] and has been assigned a new accession number, NHMAD 2020.00001. We opt to refer to this specimen as exBHI 3033 throughout the manuscript to remain consistent with prior referenced literature [10,40,58].

We compared our reconstructions in tyrannosaurs to bipedal, striding, extant animal models, including the ostrich *Struthio camelus*, the largest extant terrestrial bird [44,59], using the data from Alexander *et al.* [59]. While other extant bipeds are available for study [60], outside of avians and

Table 1. Two-dimensional measurements derived from Hartman [40,42,43], Persons & Currie [54] and Zanno & Napoli [56]. (Cross-referencing material from Hutchinson *et al.* [10]. Margins of error are at most under 3% between measurements and cross-referencing material from Hutchinson *et al.* [10].)

specimen	LACM 23845	MOR 555	exBHI 3033	FMNH PR 2081
two-dimensional measurements (complete leg)	2.558 m[b,e]	3.6 m[d]	3.61 m[a]	3.77 m[c]
two-dimensional measurements (femur, tibiotarsus and tarsometatarsus)	2.158 m[b,e]	3.1 m	3.11 m	3.25 m
cross reference (femur, tibiotarsus and tarsometatarsus)	N/A	3.055 m[f]	3.068 m[f]	3.3 m[f]

[a]Hartman [40].
[b]Persons & Currie [54].
[c]Hartman [42].
[d]Hartman [43].
[e]Zanno & Napoli [56].
[f]Hutchinson *et al.* [10].

Homo sapiens, these organisms do not use a striding gait and as such are inappropriate for study. In addition, a model *H. sapiens*, the only other clade of extant, obligate striding bipeds, was derived as an average of the dataset of Cavanagh & Kram [61]. Ratites and humans were used because they are the largest extant obligate bipeds, and differences in their gaits enable broader and more phylogenetically informed comparisons.

2.2. Specimen dimensions

Anatomical data on leg length was obtained primarily from two-dimensional reconstructions [40–43], augmented with more precise measurements with available published measurement data. Measurements were cross-referenced with data from Hutchinson *et al.* [10] to ensure accuracy. There are limitations to using two-dimensional reconstructions, as measurements often become misleading or contain some degree of error since measurements obtained from lateral view may not properly convey deviation from the sagittal plane. However, it should be noted that despite concerns in using two-dimensional reconstructions, analyses indicate little deviation from the sagittal plane in the hind limb posture of the closely related tyrannosaurid *Daspletosaurus* [44]. This reduces the potential for error in measurements taken from the lateral view of reconstructions. Differences in exact measurements between the sources were small, at an approximate 3% margin of error. Data for *H. sapiens* and *S. camelus*, sourced from Cavanagh & Kram [61] and Alexander *et al.* [59], are found in the electronic supplementary material, file S1 (table 1) .

2.3. Hip height

Hip height influences speed and locomotory estimates [17,62] and various estimates have been reported for tyrannosaurs in literature. Low hip height values, such as those suggested by Paul [8], are incompatible with fast locomotion because large moment arms place extreme demands on musculature [62]. Conversely, the highest hip heights, such as some variations by Gatesy *et al*. [62] or Bishop *et al.* [44], may present challenges in keeping the centre of mass supported by the leg [62]. We used levels of crouch derived by Hutchinson & Garcia [20] and Gatesy *et al.* [62] to calculate three estimates for hip height ranges, however, given concerns for the most extreme columnar stances, alongside the minimal variation it represents (less than 5%), we modelled several hip height ranges but excluded extremely low or high levels of crouch. A minimum hip height at 75% crouch, representing a standing hip height of 2.5 m to the proximal pedal phalanx, was derived from MOR 555. The highest hip height at 95% crouch was 3.15 m. Then, we calculated the mean between the maximum and minimum hip heights for each specimen. These values were used in creating a broad and workable dataset to facilitate analyses and comparisons, with the caveat that these mid-stance postures are not being evaluated for their ability to enable an individual's greatest locomotor performance.

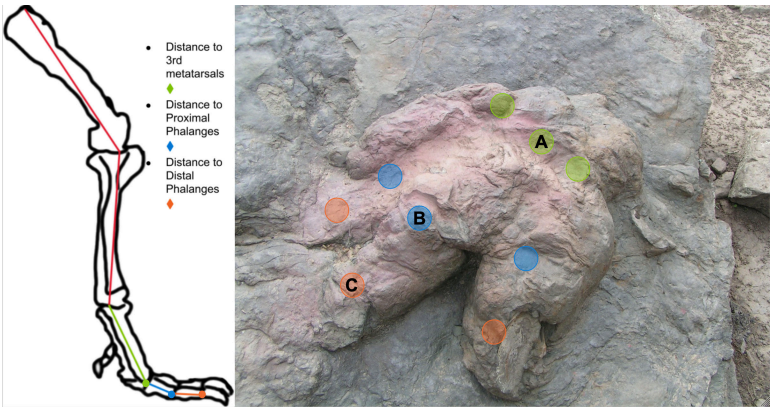

Figure 2. Measurements of a *T. rex* leg including leg length remaining in articulation with the acetabulum, distance to the third metatarsals, proximal phalanges and distal phalanges of digits I, II and III. Locations have been superimposed onto the ichnospecies *Tyrannosauripus pillmorei*. Photo by Rufus Crown-Sparrow (Wikimedia Commons), and outline of the *T. rex* leg traced from a photo by H. F. Osborn, currently housed in the public domain. Links to the original photo are provided in the electronic supplementary material, S1.

2.4. Foot-strike models

We divided the foot into three points using anatomical landmarks and points of contact with the ground (figure 2) to represent where the foot may have touched the ground first. The first point is the rear-foot or the area up to the distal portion of the third metatarsals (figure 2, point A) [63,64]. The second point is a mid-foot strike (MFS) and was measured at the distal portion of the proximal phalanges (figure 2, point B). The third point is a distal-foot strike (DFS) and was measured at the distal portion of the distal phalanges (excluding the ungual (figure 2, point C)). These terms are used in previous studies [65,66] but modified for the purposes of our study for the specifics of a digitigrade animal. In standard terminology for plantigrades such as *H. sapiens*, rear-foot strike (RFS) occurs at the calcaneum (heel), MFS at the distal metatarsals and DFS at the pedal digits [65,66].

2.5. Model parameters

2.5.1. Formulas and application

We applied three formulae equations (2.1)–(2.3) to create a range of speed and stride frequency estimates for each specimen using each combination of foot-strike pattern, relative stride length (RSL) and hip height. These formulae have been extensively applied to speed estimates for other extant and extinct animals with varying anatomy and locomotory behaviour [17–19,45,67]. As such, they present an opportunity to characterize and quantify the range of consequences for various behaviours in locomotion based on foot-strike patterns. While other equations are available [68], they do not provide information on SL, hip height, nor stride frequency, thus making their use incompatible with this analysis. For the following formulae, the variable λ reflects SL, g reflects gravity, h reflects hip height and u reflects velocity (figure 3):

$$u = 0.25g^{0.5} \times \lambda^{1.67} \times h^{-1.17} \quad \text{(Alexander 1976 [16])}, \tag{2.1}$$

$$u = \left[gh\left(\frac{\lambda}{1.8h}\right)^{2.56}\right]^{0.5} \quad \text{(Alexander } et\ al\text{. 1977 [77]; Thulborn \& Wade 1984[67])}, \tag{2.2}$$

$$u = 0.226g^{0.5} \times \lambda^{1.67} \times h^{-1.17} \quad \text{(Ruiz \& Torices 2013 [18])}. \tag{2.3}$$

Here, we define RSL as absolute SL/hip height. To establish a broad range of results, RSL values of 2.0, 2.5 and 3.0 were calculated. Generally, RSL also aligns with the transitions in gait between walking and running, with animals moving above RSL 2.0 entering slow running gaits above Froude number 1 or the fastest possible walking speed [18]. Beyond RSL 2.0, in non-walking gaits, some similar universal constants are present in quadrupeds and bipeds even if specific energetics and anatomy vary [18,62]. These constants appear in the form of increased leg swing speed, oscillation in the centre of mass,

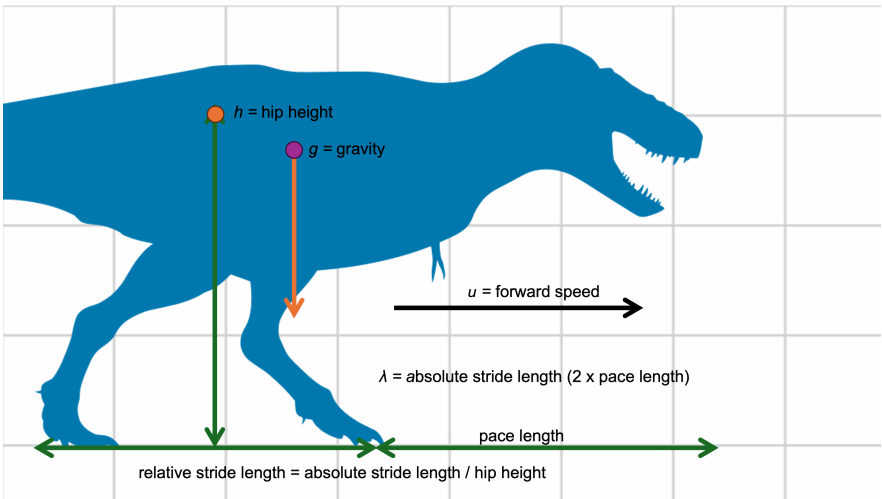

Figure 3. Visual representation of variables used. Silhouette sourced from Phylopic (Phylopic.org). Scale is 1 box = 1m. *Tyrannosaurus rex*: credit to Matt Dempsey, resized and recoloured for the purposes of comparison. Link to the original repository is provided in the electronic supplementary material, File S1.

mid-stance posture being the lowest height for the centre of mass during the gait cycle and similarly increased muscular effort [18,62]. Each SL for respective foot-strike patterns in *Tyrannosaurus* was determined by the initial point of contact for either RFS, MFS or DFS models. These ranges were selected to reflect a plausible range of SLs as described in Thulborn [18].

To establish a broad range of results, RSL values of 2.0, 2.5 and 3.0 were calculated. Each SL was determined by the initial point of contact for either RFS, MFS or DFS models. RSL can also provide an absolute SL by multiplying the used point of contact or hip height by the actual RSL, thus retrieving the actual SL. Alongside the formulae used to calculate speed, stride frequency can be derived from the calculated speed and SL.

Thulborn [18] suggests that the use of the mean of equations (2.1) and (2.2) for RSL between 2.0 and 2.9 can produce results that adhere to some animals moving above a RSL of 2.0. These results were also calculated. Additional attention must be given to equation (2.2) and its original use for running quadrupedal animals [45]. The use of this formula for dinosaurs was expanded upon by Thulborn & Wade [67] and Thulborn [18], both deeming it appropriate to use the derived formula for bipedal animals in a running gait, with emphasis placed on the importance of a gait faster than conventional walking, citing key similarities in non-walking gaits across different clades [18,67]. Specifically, despite the differences between quadrupeds and bipeds in anatomy and their energetics of running, the locomotion of quadrupeds and bipeds converge in results above RSL = 2.0 [15]. Given this convergence of applicability and the use of equation (2.2) by other studies [18,67], we apply equation (2.2) to bipeds with caution.

2.5.2. Model validation and justification: empirical observation and modelled result accuracy

To assess the validity of our model, we (i) established that if exact parameters of hip height and stride frequency and appropriate equations for the RSL were used, then the produced results should align with direct observation in living species to a reasonable degree. Then, (ii) we established that the equations are sensitive enough to detect changes in results across various foot-strike patterns in living species where these consequences have been observed. For the first requirement, the model *S. camelus* and *H. sapiens* with information sourced from Alexander *et al.* [45], with data for the birds *Dromaius novaehollandiae*, *Meleagris gallopavo, Porphyrio porphyrio, Coturnix chinensis, Colinus virginianus*, as well as additional specimens of *S. camelus* and *H. sapiens* using slower gaits from Bishop *et al.* [44], were used as points of comparison between the results of equations (2.1)–(2.3) and empirical observation. This analysis tested the ability of the formulas to produce results in-line with empirical, observed results. The empirical observations and the closest results produced by equations (2.1)–(2.3) are displayed in figure 4. Aligning with Marmol-Guijarro *et al.* [69], calculated results for small birds possessed significant ranges of error, in some cases more than 60%. Contra Marmol-Guijarro *et al.* [69] results for animals with larger body sizes produced nearly exact matches. This indicates that while equations

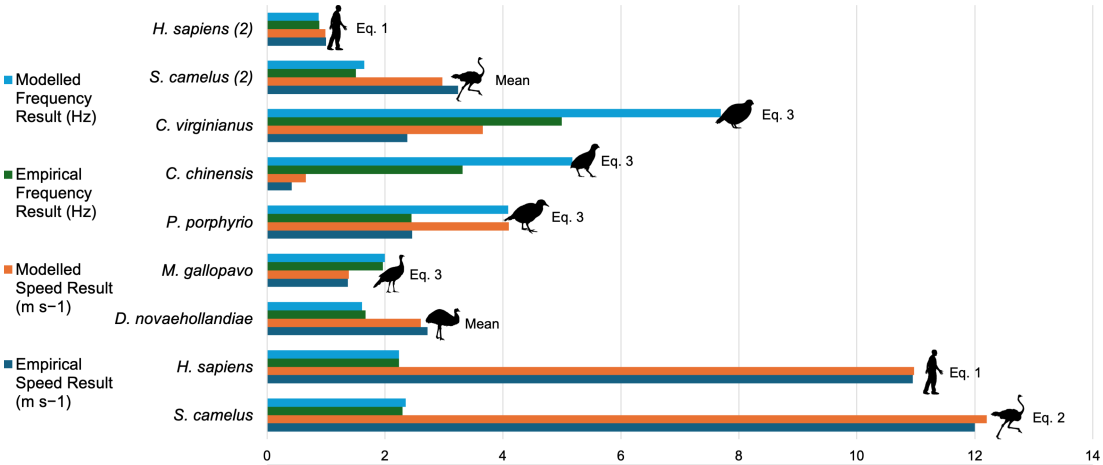

	S. camelus	H. sapiens	D. novaehollandiae	M. gallopavo	P. porphyrio	C. chinensis	C. virginianus	S. camelus (2)	H. sapiens (2)
Modelled Frequency Result (Hz)	2.35	2.24	1.612	1.996	4.088	5.177	7.693	1.652	0.879
Empirical Frequency Result (Hz)	2.3	2.236	1.67	1.967	2.451	3.315	4.999	1.509	0.888
Modelled Speed Result (m s−1)	12.2	10.97	2.61	1.39	4.1	0.66	3.66	2.97	0.99
Empirical Speed Result (m s−1)	12	10.95	2.72	1.37	2.46	0.42	2.38	3.24	1

Figure 4. Comparison of empirical observed results and modelled results from equations (2.1)–(2.3) for speed and stride frequency to test the models' ability to produce accurate results. Animals with a mass of greater than 1 kg usually had a formula available which produced results with less than 10% error. Silhouettes sourced from Phylopic (Phylopic.org), *S. camelus*: credit to Ferran Seyol; *H. sapiens*: Andrew Farke; *Colinus virginiaus*: Gabriela Palomo-Munoz; *Coturnix coturnix* (stand in for *C. chinensis*): Marie-Aimée Allard; *Gallirallus australis* (stand in for *P. porphyrio*): T. Michael Keesey and HuttyMcphoo; *M. gallopavo*: Gabriela Palomo-Munoz; *D. novaehollandiae*: Andy Wilson. Links to the original repository are provided in the electronic supplementary material, S1.

(2.1)–(2.3) are not calibrated for small animals, sampling large bipeds of greater than 1 kg suggests that at minimum one formula can produce accurate results with a margin of error below 10%. Generally, mean results of equations (2.1) and (2.2) produced the most accurate results for large ground birds moving with an RSL below 2.0, while equation (2.2) produced the most accurate results for any animal moving with an RSL at or above 2.0. This is in-line with evidence of birds moving with elevated stride frequencies at lower RSLs [38,44].

2.5.3. Model validation and justification: model and equation sensitivity to changes in foot-strike pattern

The second requirement—establishing that the equations are sensitive enough to detect changes in results across various foot-strike patterns in living species where these consequences have been observed—was tested using *H. sapiens* and *S. camelus* models because we have exact data for their leg dimensions. Equations (2.1)–(2.3) were used alongside an intermediate hip height and a RSL of 2.0–3.0, alongside all three foot-strike patterns; RFS, MFS and DFS. Searches were performed for speed and stride frequency. In total, 54 results were produced for speed and 54 individual results were produced for stride frequency, with an additional 108 results for both speed and stride frequency produced at different hip heights, totalling 162 results for speed and stride frequency (electronic supplementary material, file S1). Differences in stride frequency were marginal but overwhelmingly consistent in their presence between different foot-strike patterns (figure 5).

2.5.4. Model sensitivity analysis: extinct taxa margin of error

To identify potential range of error in extinct taxa, each formula had the inputs of SL and hip height changed to identify differences in speed and, consequently, stride frequency. We sampled *T. rex* specimen MOR 555 with each equation. Inputs of hip height were increased by 5%, 10% and finally 15%, respectively. Our methodology represents an idealized approach and focuses on controllable variables within a range of plausible values with the outcomes being testable with further experimental data gathered from extant animals. We do note, however, that this precision is almost certainly impossible to extend to non-idealized field settings, as outlined in Marmol-Guijarro *et al.* [69]. Expected error in measurements is approximately 3% (table 1) within the measurements themselves and hip

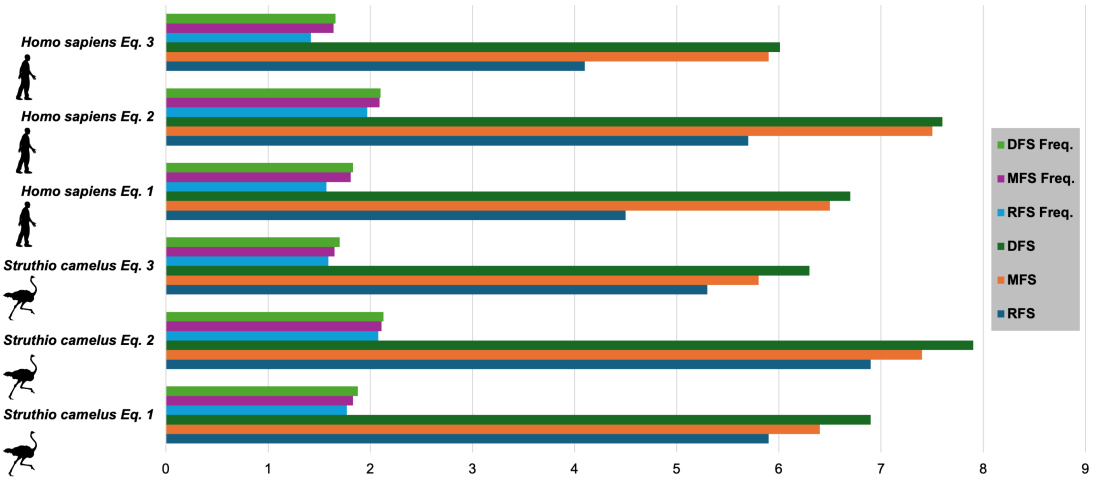

	Struthio camelus Eq. 1	Struthio camelus Eq. 2	Struthio camelus Eq. 3	Homo sapiens Eq. 1	Homo sapiens Eq. 2	Homo sapiens Eq. 3
DFS Freq.	1.88	2.13	1.7	1.83	2.1	1.66
MFS Freq.	1.83	2.11	1.65	1.81	2.09	1.64
RFS Freq.	1.77	2.08	1.59	1.57	1.97	1.42
DFS	6.9	7.9	6.3	6.7	7.6	6.01
MFS	6.4	7.4	5.8	6.5	7.5	5.9
RFS	5.9	6.9	5.3	4.5	5.7	4.1

Figure 5. Sensitivity analysis of stride frequency and speed between foot-strike patterns, in extant bipeds *S. camelus* and *H. sapiens*. MFS and DFS patterns produced higher speed results and stride frequencies than RFS patterns. Silhouettes sourced from Phylopic (Phylopic.org), *S. camelus*: credit to Ferran Seyol, *H. sapiens*: Andrew Farke. Links to the original repository are provided in the electronic supplementary material, S1.

height could vary up to 10%, assuming the most columnar stances are viable [44,62]. We note that if the result of a hip height is potentially skewed, the entire dataset would change as well by consistently shifting the relevant spread of results calculated with that hip height.

2.6. Statistical analysis

To ensure consistency, we calculated 100 results of speed and stride frequency for each equation (equations 2.1–2.3 and means of equations 2.1 + 2.2). Variables in the results were comprised individual specimens, foot-strike pattern, equations used, hip height and RSL outlined in methods. In turn, SL/hip height, λ/h, is calculated for each speed result, in turn producing over 100 additional results for λ/h. Alongside reporting percentage differences, two Kruskal–Wallis tests were performed in R-Studio using the MultNonParam and dunn.test packages to test the significance of results in speed and stride frequency. Additional testing was done with a post hoc Dunn's test using an alpha of 0.05 and Bonferroni corrected alpha of 0.017. A non-parametric test was used since normal distribution among speed and stride frequency could not be assumed.

3. Results

3.1. Model sensitivity analysis: extinct taxa margin of error

Results for *Tyrannosaurus* specimen MOR 555 revealed that equations (2.1) and (2.3) were typically the most vulnerable to variation and produced the most significant shifts in results with changes in the actual input. The highest recorded input was found in equation (2.3) at RSL 2.0, with a 15% increase in hip height resulting in a 20% margin of error. More typically, at a 15% inferred error in the input, equation (2.1) produced a range of error at 15% while equation (2.2) produced a range of error at 13%. At the lowest introductory rate of error, a margin of 5%, error ranges fell between 3% and 7% error. Equation (2.2) produced the lowest error, mean results and equation (2.1) produced intermediate results in this range, while equation (2.3) possessed the highest margin of error. With the margin of error in hip height being at most 3% within the measurements themselves, we can expect the most precise margins of error in results of stride frequency and speed to be less than 6.5%, with expected margins of error at 2.4% for speed results and 4.6% for frequency results (figure 6).

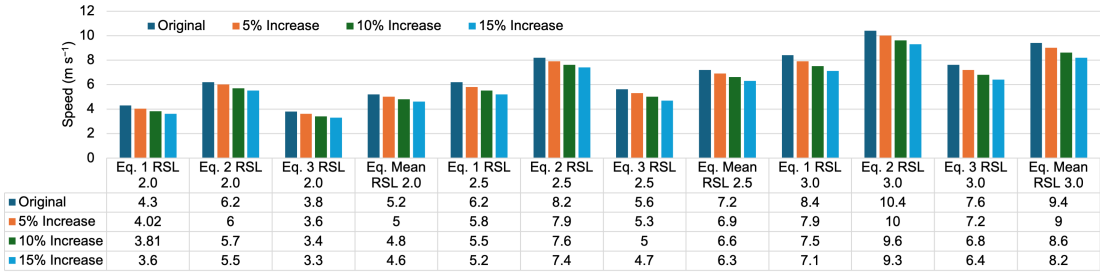

	Eq. 1 RSL 2.0	Eq. 2 RSL 2.0	Eq. 3 RSL 2.0	Eq. Mean RSL 2.0	Eq. 1 RSL 2.5	Eq. 2 RSL 2.5	Eq. 3 RSL 2.5	Eq. Mean RSL 2.5	Eq. 1 RSL 3.0	Eq. 2 RSL 3.0	Eq. 3 RSL 3.0	Eq. Mean RSL 3.0
Original	4.3	6.2	3.8	5.2	6.2	8.2	5.6	7.2	8.4	10.4	7.6	9.4
5% Increase	4.02	6	3.6	5	5.8	7.9	5.3	6.9	7.9	10	7.2	9
10% Increase	3.81	5.7	3.4	4.8	5.5	7.6	5	6.6	7.5	9.6	6.8	8.6
15% Increase	3.6	5.5	3.3	4.6	5.2	7.4	4.7	6.3	7.1	9.3	6.4	8.2

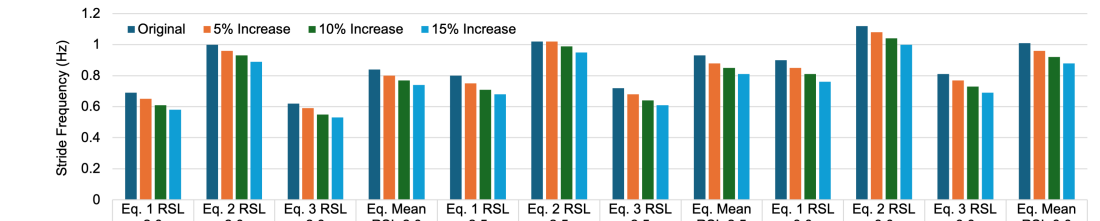

	Eq. 1 RSL 2.0	Eq. 2 RSL 2.0	Eq. 3 RSL 2.0	Eq. Mean RSL 2.0	Eq. 1 RSL 2.5	Eq. 2 RSL 2.5	Eq. 3 RSL 2.5	Eq. Mean RSL 2.5	Eq. 1 RSL 3.0	Eq. 2 RSL 3.0	Eq. 3 RSL 3.0	Eq. Mean RSL 3.0
Original	0.69	1	0.62	0.84	0.8	1.02	0.72	0.93	0.9	1.12	0.81	1.01
5% Increase	0.65	0.96	0.59	0.8	0.75	1.02	0.68	0.88	0.85	1.08	0.77	0.96
10% Increase	0.61	0.93	0.55	0.77	0.71	0.99	0.64	0.85	0.81	1.04	0.73	0.92
15% Increase	0.58	0.89	0.53	0.74	0.68	0.95	0.61	0.81	0.76	1	0.69	0.88

Figure 6. Sensitivity analysis of *Tyrannosaurus* specimen MOR 555, using different hip heights which may reflect anticipated error within used measurements.

3.2. Speed results: all specimens of *Tyrannosaurus rex*

As the foot-strike pattern shifted to more distal elements of the pes, top speed increased. Top speed was slowest in the RFS model, intermediate speeds used the MFS model and the fastest results used the DFS model. The average difference in speed between RFS and DFS models averaged approximately 20% across all datasets and inputs. When using the lowest values from the dataset, the speed difference between RFS and DFS models increased to approximately 42% (table 2). The largest values in the dataset produced an average difference of approximately 15%, indicating that higher speeds may have a stabilizing effect on the per cent difference. Critically, this percentage of variation is greater than the margin of error anticipated by the sensitivity analysis. The variation of speed with foot-strike patterns was also influenced by RSL, with a higher RSL producing more divergence between speed results, even when all variables excluding foot strike were identical. Functionally, the change in point of contact results in the absolute SL increasing more than the standing hip height might suggest. This effect is most prominent in the smaller LACM 23845 which would be less constrained by the need for extremely columnar poses and, in turn would have a greater functional leg length compared to hip height [37]. The discrepancy between functional leg length and hip height is noticeable in even the most proximal foot-strike patterns.

The Kruskal–Wallis H test indicated a statistic of 21.0466 (outside 95% region of acceptance: [0, 5.9915]) and p-value of 0.0000269, below the threshold of significance at $p = 0.05$, for speed, between the different groups ($\chi^2_2 = 21.05$, $p < 0.001$). Mean rank scores were 180.82 for RFS, 220.76 for MFS and 247.92 for DFS, respectively. The post hoc Dunn's test using an alpha of 0.05 indicated that the mean rank of the following pair is significant: RFS–DFS. Testing was repeated with a Bonferroni corrected alpha of 0.017, again indicating significant difference in RFS–DFS. With the rejection of the null hypothesis, it can be concluded that foot-strike pattern has a significant effect on speed (figure 7).

3.3. Stride frequency results: all specimens of *Tyrannosaurus rex*

Stride frequency consistently increased with more DFS patterns. RFS patterns produced the lowest stride frequencies, MFS patterns produced intermediate stride frequencies between RFS and DFS patterns and DFS patterns produced the highest stride frequencies. This change was the most pronounced at higher RSL, such as RSL 2.5 and 3.0. Additional variation and significance of the difference also varied between formulae and became less pronounced in individual data points for larger animals like exBHI 3033 and FMNH PR 2081 (see the electronic supplementary material, S1).

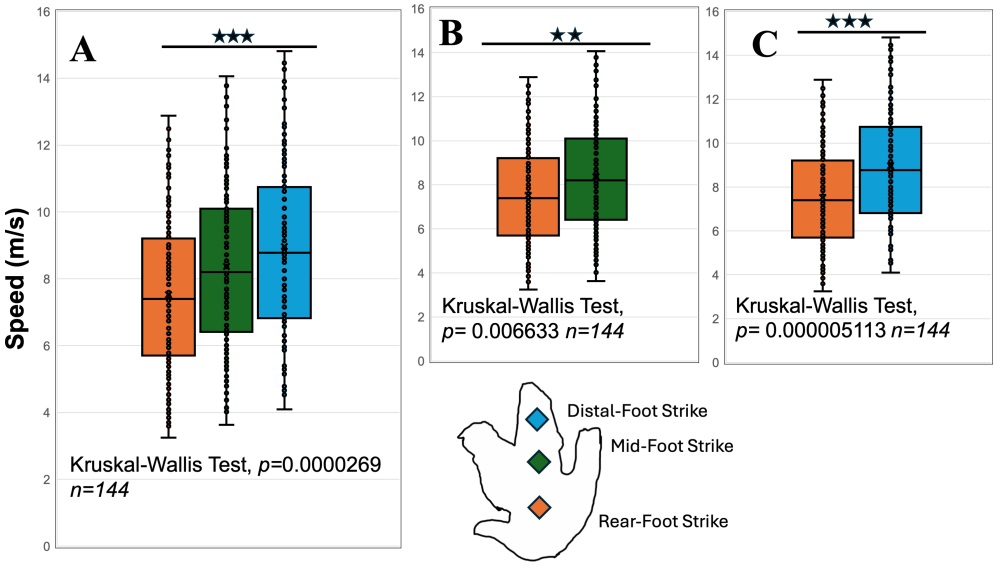

Figure 7. A comparison of foot-strike patterns and speed. Each foot-strike pattern is included, using each equation, each hip height and each RSL. More DFS patterns result in higher top speeds. (A) RFS, MFS, DFS comparison ***$p = 0.0000269$, (B) RFS and MFS comparison **$p = 0.006633$, (C) RFS and DFS comparison ***$p = 0.000005113$. Outline of ichnospecies *T. pillmorei* modified from Lockley & Hunt [31].

Table 2. Differences between RFS and DFS values across average, maximum and minimum values in the complete dataset. RFS–DFS is highlighted to compare the traditional foot-strike pattern in previous studies to the best supported foot-strike pattern based on recent analyses. * Signifies significance.

input	% difference RFS–DFS, avg. values	% difference RFS–DFS, max. values	% difference RFS–DFS, min. values
equation (2.1)	7.0–8.5 m s^{-1}, 21%	11.4–13.7 m s^{-1}, 20%	3.6–4.5 m s^{-1}, 26%
equation (2.2)	8.8–10.2 m s^{-1}, 16%	12.9–14.8 m s^{-1}, 15%	5.2–6.2 m s^{-1}, 19%
equation (2.3)	6.3–7.7 m s^{-1}, 21%	10.3–12.4 m s^{-1}, 17%	3.2–4.1 m s^{-1}, 26%
mean	7.9–9.4 m s^{-1}, 19%	12.2–14.3 m s^{-1}, 17%	4.4–5.4 m s^{-1}, 22%
average	20% increase	18% increase	23% increase
***p*-values, Kruskal–Wallis**			
comparison (RFS, MFS, DFS)* **	**RFS–MFS****	**RFS–DFS*****	**MFS–DFS**
0.0000269***	0.006633**	0.000005113***	0.06498

These results broadly align with allometry-based predictions [70]. The trend of increasing stride frequency holds between equations (2.1)–(2.3) and means of equations (2.1) + (2.2), showing that this trend is not an individual discrepancy from a single formula.

Distal-foot strike patterns produced the highest stride frequencies, MFS patterns produced intermediate stride frequencies and RFS models produced the lowest stride frequencies. Increases of stride frequency between the foot-strike patterns are typically less than 10%, with the largest discrepancy of stride frequency between DFS and RFS patterns. An average increase of 8% or typically 0.1–0.09 Hz is found between RFS and DFS patterns; the greatest values averaging percentile differences between DFS and RFS patterns of 5% or 0.1 Hz, while the smallest values also average a difference of 5% with a difference of 0.03 Hz (table 3). This difference broadly exceeds the conservative margins of error anticipated by the more limited range of error within inputs that could be expected. The effect on absolute SL does not appear significant, with an additional Kruskal–Wallis H test retrieving a non-significant difference in the dependent variable between the different SLs, $\chi^2_2 = 1.14$, $p = 0.564$, with a mean rank score of 24.5 for RFS, 27.94 for MFS and 30.06 for DFS.

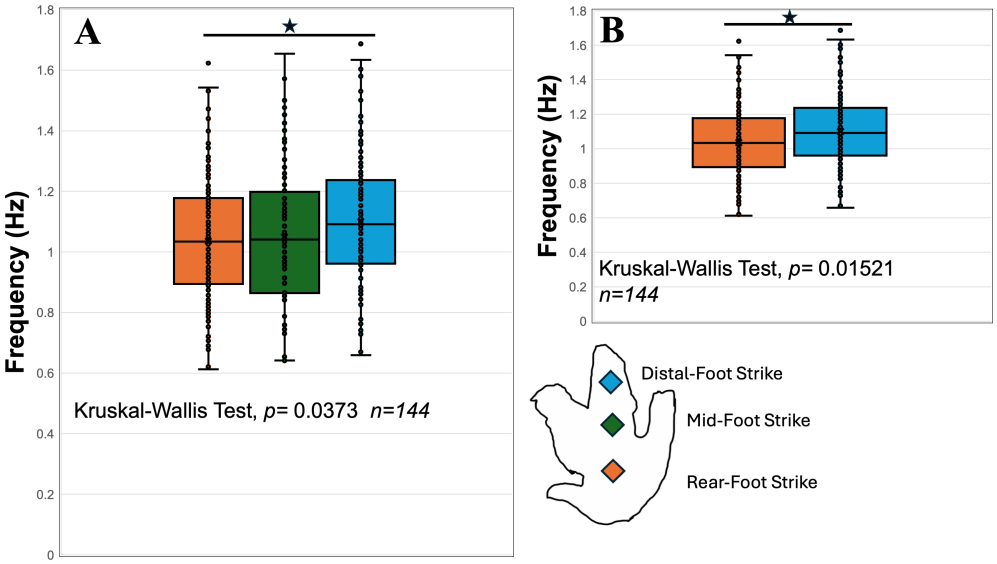

Figure 8. A comparison of foot-strike patterns and stride frequency. Each foot-strike pattern is included, using each equation, each hip height and each RSL. More DFS patterns result in higher stride frequencies. (A) RFS, MFS, DFS comparison *$p = 0.0373$, (B) RFS and DFS comparison *$p = 0.01521$. Outline of ichnospecies *T. pillmorei* modified from Lockley & Hunt [31].

Table 3. Differences between RFS and DFS values across average, maximum and minimum values in the *T. rex* dataset. (RFS–DFS is highlighted to compare the traditional foot-strike pattern in previous studies to the best supported foot-strike pattern based on recent analyses. *Signifies significance.

input	% difference RFS–DFS, avg. values	% difference RFS–DFS, max. values	% difference RFS–DFS, min. values
equation (2.1)	0.96–1.04 Hz, 8%	1.44–1.58 Hz, 10%	0.68–0.73 Hz, 8%
equation (2.2)	1.22–1.26 Hz, 3%	1.62–1.69 Hz, 4%	0.98–1.01 Hz, 3%
equation (2.3)	0.87–0.94 Hz, 8%	1.30–1.43 Hz, 10%	0.61–0.66 Hz, 8%
mean	1.09–1.15 Hz, 5%	1.53–1.63 Hz, 7%	0.83–0.87 Hz, 5%
average	6% increase	8% increase	6% increase

Kruskal–Wallis *p*-values			
comparison (RFS, MFS, DFS)*	RFS–MFS	RFS–DFS*	MFS–DFS
0.0373*	0.6195	0.01521*	0.05351

The Kruskal–Wallis H test indicated a statistic of 6.5776 (outside 95% region of acceptance: [0, 5.9915]) and p-value of 0.0373, below the threshold of significance at $p = 0.05$, for stride frequency, between the different groups ($\chi^2_2 = 6.58$, $p = 0.037$). Mean rank scores were 202.16 for RFS, 209.47 for MFS and 237.88 for DFS, respectively. The post hoc Dunn's test using an alpha of 0.05 indicated that the mean rank of the following pair is significant: RFS–DFS. Testing was repeated with a Bonferroni corrected alpha of 0.017, indicating significant difference in RFS–DFS. With the rejection of the null hypothesis, it can be concluded that foot-strike pattern has a significant effect on stride frequency (figure 8).

4. Discussion

The results of these data indicate that limiting a model to striking the ground with the proximal portions of the foot, or not considering where or when the broader pes anatomy contacts the ground, results in noticeable and consistent reductions in stride frequency. At present, the best-supported foot-strike patterns for *Tyrannosaurus* involve the distal-foot based on present trackway analysis of other theropods and analyses of other tyrannosaur trackways. This includes Jurassic ichnotaxa

assignable to modestly sized theropods probably encompassing a broad swath of animals from coelurosaurs and other theropod clades [28–30,36]. Additional support for these foot-strike kinematics and DFS patterns is imparted by the foot's functional morphology [23,24].

The results of this study and assessment of previous literature further elucidate the significance of DFS patterns and why they more effectively function in tandem with the functional morphology of the pes. Previous two-dimensional and three-dimensional models [58,71] and qualitative discussion [63,64] reconstructing tyrannosaur locomotion have assumed the foot-strike pattern is 'proximal-first', and thus striking the ground with their distal metatarsals for the gait of *T. rex*. This is inconsistent with what has been directly observed from trackways associated with large tyrannosaurs, modern birds and other theropods [28–30,36]. Furthermore, 'proximal-first' models may compromise ligamentous shifting of stress [25] away from the gracile proximal splint third metatarsal, limiting the amount of force the skeleton could withstand and reducing locomotor performance [22–25]. Finally, proximal-first striking is at-odds with evidence from bipedal locomotory models of both birds [37,38,44] and human athletes [66] which use distal foot elements resulting in more effective running both in terms of kinematics and linear speed [66]. Therefore, changes in reconstructed locomotion, including gait, gait transitions, speed, kinematics, metabolic energy cost and stress applied to hindlimb elements during the gait cycle, are anticipated if the foot functioned analogously to that of birds, and potentially allowing for more bird-like running. The results of this study in finding that bird-like DFS patterns result in higher stride frequencies and moderately elevated top speeds, indicate that this change in reconstructed locomotion does facilitate more bird-like running.

Critically, there appears to have been a significant degree in which theropod foot kinematics are conserved, even in non-coelurosaurs lacking the arctometatarsalian condition [29,36]. We do note, though, that theropod trackways including those of tyrannosaurs do not appear to have a strong degree of pronation or 'pigeon-toed' effect [29,36]. Although pronation probably shifts force distribution in the hindlimb [72], pronation does not appear to shift foot-strike patterns given that extant birds even with a 'pigeon-toed' condition still use DFS patterns [28,30]. Detailed reconstructions of track formation on various substrates both in avians [28,30] and extinct dinosaurs [29,36] show a 'toe-first' or DFS pattern reinforcing this behaviour being widespread among most if not all Theropoda, including *T. rex*. This probably holds significant consequences for the evolution of Theropoda and aves, with the potential to also outline key locomotor differences between ornithodirans and other archosaurs.

The rejection of the null hypothesis, that foot-strike pattern does not affect speed or stride frequency, in this study further suggests that *T. rex*, a derived coelurosaur, was moving more like its avian relatives with DFS patterns, elevated stride frequencies, shorter RSL and presumably the potential for faster locomotory speed estimates [37,38,44]. This would align with some qualitative discussion of the leg and especially the foot being described as bird-like [6–8], although these assertions are severely hampered by their lack of quantitative backing.

4.1. Speed results and interpretations

The speed of *Tyrannosaurus* has been of keen interest ever since its discovery and early years of study [15,73]. Currently, most quantitative studies support a slower gait [20,58,68], rather than the faster interpretations derived from qualitative analyses [6–8]. Key limiting factors in the speed of *T. rex* are its ability to support the forces required for high-speed running beyond 11 m s^{-1} [20,62,74], sufficient muscular power and stored energy [68,75] and stresses exerted on bones [58]. In summary, this results in a cited range of 5–11 m s^{-1} [20].

When trying to identify what speed the sampled *Tyrannosaurus* specimens should be moving at several things must be considered. As established by the results of this study and past literature, DFS patterns and equations favouring high stride frequency are most likely [28,29]. To enable suspended phase running, the most columnar hip heights would be required for adult *T. rex*, while smaller, younger animals would be less constrained [62]. In terms of RSL, based on limitations of force generation capacity and behaviour of extant bipeds [37,38,44], it is likely that older, heavier animals moved with a lower RSL, while younger animals could use a higher RSL. The results produced using the most accurate possible inputs broadly fall within the range of previous quantitative studies [20,68,71,76,77]. Recent mass estimates suggest that many of these animals may be heavier and slower [14]. Our results indicate adult *T. rex* specimens at different masses would move at noticeably different speeds. Particularly with adults, the difference in speed between the 6.5 tonne MOR 555 moving at 9.5 m s^{-1} [62] compared to the 9.5 tonne FMNH PR 2081 moving at 6.3 m s^{-1} [10] probably means these size classes of animals preyed upon different animals [50]. Notably, massive adult *T. rex* such as FMNH

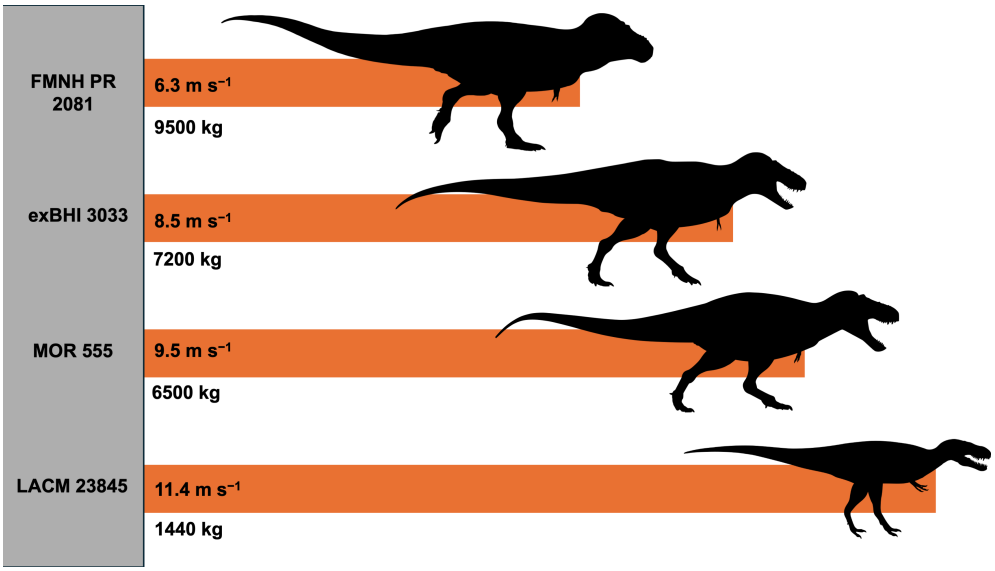

Figure 9. Estimated speeds of *T. rex* specimens in the dataset. Silhouettes sourced from Phylopic (Phylopic.org). Top: *T. rex*, credit to Jack Meyer Wood; second from top: *T. rex*, credit to Matt Dempsey; third from top: *T. rex*, credit to Manuel Brea Luerio; bottom: *T. rex*, credit to Conty. Links to the original image repository are provided in the electronic supplementary material, S1.

PR 2081 would have passed through the same mass range as smaller specimens of *T. rex* as they grew, and by consequence would have hunted multiple different kinds of animals during their lifetime. At present, the results of this study present no reason to suspect adult *T. rex* could move faster than this general range.

We also note that higher speeds found in younger, smaller animals such as LACM 23845 (figure 9), lends further support to ontogenetic niche separation [49,50,78]. With the recognition of *Nanotyrannus* as a distinct taxon [56], the pronounced changes in locomotor capability between mature and immature *Tyrannosaurus* become interesting under the lens of ecology. Although hindlimb proportions between *Nanotyrannus* and immature *T. rex* differ, particularly in the femur and tibia, total leg length is similar [54]. This may indicate similar locomotor performance and a similar bird-like gait within the observed patterns of reported measurements (electronic supplementary material, file S1). The presence of two relatively fast multi-hundred-kilogram predators [56], *Nanotyrannus* and immature *T. rex*, merits further analysis in ecological niche partitioning and the environmental circumstances which supported these predators.

4.2. Similarities and differences: *Tyrannosaurus*, birds and other bipeds

Significant divergence between running in avians and humans is well-known, with emphasis on ground contact time, elevated stride frequencies and smoother transitions between walking and running gaits defining avian running [37,38,44,79]. While ground contact time remains important for all running birds, size is critical in aspects of running kinematics. Larger birds place increased emphasis on stride frequency alongside lower duty factors with proportionally shorter strides, and in turn enter a run at lower SLs in a similar smooth manner to other birds [38,44]. We also note that the largest ratites are faster than humans [59].

Elements of this style of locomotion have been recovered in *Tyrannosaurus*. In Sellers *et al.* [58], variations around the 200 MPa bone stress limit produced a running *T. rex* moving with an elevated stride frequency and short RSL. Additionally, the ankles and feet were extensively bound by ligamentous connections [24,26], and recent work also suggests that elasticity of ankle extensor tendons has been under-considered [80]. DFS patterns would probably present a larger surface area on contact with the ground during the catch and launch phases of the stride cycle. Alongside increased cartilage [81–83], these factors may reduce stresses on the feet and metatarsals which were previously recovered as a limiting factor and increase capacity to support a high ground reaction force [20,58,62,74]. The role of distal points of contact supporting elevated stride frequencies therefore probably lends further support to the hypothesis of *T. rex* moving like a non-volant avian. Notably, increased stride frequencies without significant increases in relative SL and moderately increased top speeds would also imply

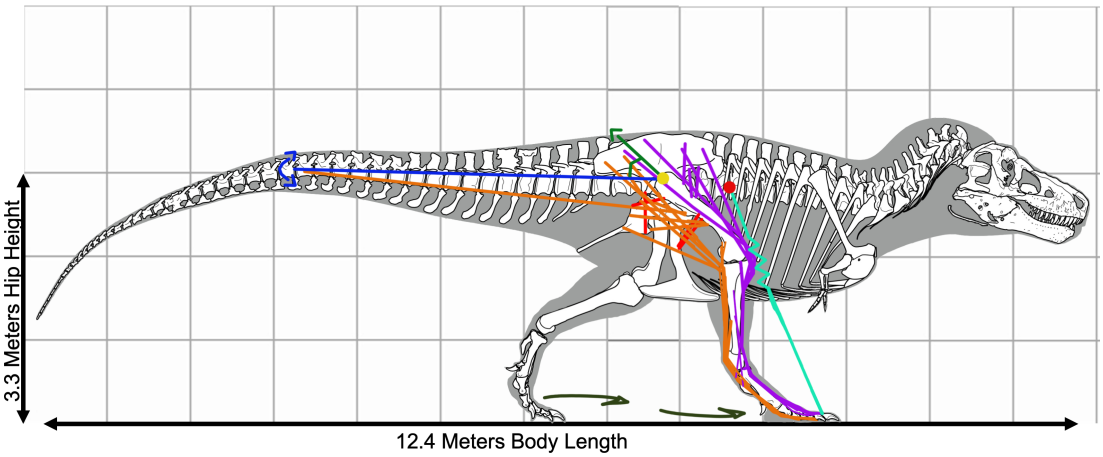

Figure 10. Visual representation of some of the key aspects of future models of *Tyrannosaurus* locomotion complementing Sellers *et al.* [58], including an oscillating, dynamic tail, alongside a more bird-like foot function and up-to-date muscle distribution. Such a model and its results of how *T. rex* moved and how fast it moved would be key to understanding how *T. rex* functioned as an apex predator and acquired prey animals as confirmed by the fossil record. Scale is 1 box = 1 m. Original image and credit belong to Dr Mark P. Witton; modified with permission.

emphasis on rapid changes in the position of the centre of mass, the body and hindlimbs, indicative of bird-like running [37].

Despite similarities between *Tyrannosaurus* and extant avians, a significant documented divergence between *T. rex* and its modern relatives is the tail and general function of the hip [11,13,84–86]. Whereas the role of the femur is reduced in avians with more distal elements such as the knee playing a greater role in locomotion, the hip and femur played a much more significant role in the locomotion of non-avian theropods [11,74,79,85]. One of the most significant contributors to this discrepancy is the presence of the tail, which plays a key role in femoral retraction, energy storage and energetics [11,84]. The presence or absence of a heavily muscled tail which plays a key role in femoral retraction has been shown to have a significant effect on locomotion [11,39,84,87]. Even with the proportionally shortened tail of a coelurosaur compared to other theropods, the presence of a heavily muscled tail represents a point of divergence between *T. rex* and its modern avian relatives in the role of the hip. An additional point must also be made for limitations in the ankle, with previous literature recovering the ankle of *T. rex* as less muscled than its closest extant relatives, avians [10,74]. This point may be revisited by future studies given the close relationship between *T. rex* and its close relatives and the significant discrepancy between the extensor muscle mass in the ankles [88].

4.3. Limitations and future directions

While we have made reasonable efforts to control error, ensure model accuracy and perform statistical analyses, challenges remain. We have demonstrated that the foot functioned in a bird-like manner with elevated stride frequencies, and in turn probably contributing to a bird-like gait, the ability of our models to allow the foot and large, muscular tail to properly interact may be in question. Although it has been established by recent studies that equations derived from empirical observations are useful in understanding extinct taxa [68,89], this does not guarantee results with the high accuracy we would want. Additionally, while we have validated the use of equations (2.1)–(2.3) in artificial settings, we hesitate to assert that similar analysis can be performed on fossil trackways, given previously outlined concerns [69]. We may have stronger indications of how a *T. rex* moved, with a bird-like foot movement and powerful musculature enabling high stride frequencies in conjunction with lower RSL alongside similar characteristics of bird-like running [37,38,44]. However, this is not the high level of fidelity needed to produce the most definitive results. In summary, our work represents an effort to examine what insight might be gained via the creation of a broad and easily workable dataset and in turn how these results may be used to inform future models.

Future directions to explore include similar analyses on other theropods across a broader phylogenetic range, identifying when this bird-like foot function may have appeared within Dinosauria. Additionally, quantitative results within our dataset provide evidence of bird-like running defined by

high stride frequencies and DFS patterns, presenting a new approach to modelling a moving animal. DFS patterns would present more surface area on contact with the ground, and alongside evidence of stabilizing ligaments and increased musculature [26,80] would probably alleviate the pressure on foot and ankle, identified as limiting factors for running gaits in some simulations [58]. Ideally, we could see a three-dimensional model incorporating the results of this study alongside musculature and arthrology in-line with extant relatives [24,26,74,80] as well as a more dynamic model with an oscillating tail, similar to analyses performed in Bishop *et al*. [84] and van Bijlert *et al*. [86] (figure 10). A more accurate model restoring how *T. rex* moved and how quickly it moved would be vital in understanding the predatory function of *T. rex*, allowing us to accurately understand how it acquired the prey animals fossil evidence confirms they hunted [4,5,16,71,90].

5. Conclusion

Our study represents, to our knowledge, the first quantitative biomechanical analysis of the effects of foot-strike patterns on the gait of *Tyrannosaurus*. We find that the pes of *T. rex* functioned similarly to the foot of a bird. This includes the adoption of bird-like characteristics in the gait of *T. rex*, including higher stride frequencies, proportionally short SLs and moderately elevated top speeds. This kind of locomotion would represent a significant shift in our understanding of how *T. rex* moved. It is likely that future analyses will need to be undertaken into what this may mean for other key aspects of locomotion such as top speed when additional variables are considered. It is evident that the foot of *T. rex* was of key importance to the animal, bound tightly by ligaments and demonstrating the arctometatarsalian condition. Given the importance of the foot-fall kinematics in *T. rex*, it would be fitting that future models place a high degree of emphasis on this structure.

Ethics. This work did not require ethical approval from a human subject or animal welfare committee.

Data accessibility. Raw data can be accessed via the uploaded electronic supplementary material under the name 'Supplementary_File_S1' [91]. Raw data can be uploaded into R Studio, with packages MultNonParam and dunn.test being available for installation and use.

Declaration of AI use. We have not used AI-assisted technologies in creating this article.

Authors' contributions. A.T.B.: conceptualization, data curation, formal analysis, investigation, methodology, project administration, supervision, validation, visualization, writing—original draft, writing—review and editing; K.A.-W.: conceptualization, formal analysis, supervision, writing—review and editing; J.L.K.: conceptualization, project administration, supervision, visualization, writing—review and editing; S.S.: conceptualization, data curation, formal analysis, investigation, methodology, project administration, supervision, validation, visualization, writing—original draft, writing—review and editing.

All authors gave final approval for publication and agreed to be held accountable for the work performed therein.

Conflict of interest declaration. We declare we have no competing interests.

Funding. No funding has been received for this article.

Acknowledgements. The authors would like to extend special thanks to D. Feldman, D. Hone, J. Bourke, A. Biewener, T. P. Van Der Linden, M. R. Forcellati, E. V. O'Callaghan, C. Boisvert, W. J. Hart, C. Boeye, H. Boeye, P. S. Druckenmiller, as well as E. Snively for their support and highly insightful feedback on earlier drafts of this work. The authors would also like to extend additional thanks to M. Bäker for his extremely insightful discussion on the need for more dynamic models in gaining better understandings of *T. rex*, and an additional thanks to M. Witton for allowing the use and modification of his excellent skeletal of FMNH PR 2081.

Dedication. We dedicate this manuscript to one of the authors, S. Swann, who passed away during the creation of this manuscript.

References

1. Gauthier J, De Queiroz K. 2001 Feathered dinosaurs, flying dinosaurs, crown dinosaurs and the names 'Aves'. In *New perspectives on the origin and early evolution of birds: Proc. of the Int. Symp. in honor of John H. Ostrom* (eds J Gauthier, K Querioz), pp. 7–41. New Haven, CT: Peabody Museum of Natural History, Yale University.
2. Benson RBJ, Hunt G, Carrano MT, Campione N. 2018 Cope's rule and the adaptive landscape of dinosaur body size evolution. *Palaeontology* **61**, 13–48. (doi:10.1111/pala.12329)
3. Brusatte SL, O'Connor JK, Jarvis ED. 2015 The origin and diversification of birds. *Curr. Biol.* **25**, R888–R898. (doi:10.1016/j.cub.2015.08.003)
4. Carbone C, Turvey ST, Bielby J. 2011 Intra-guild competition and its implications for one of the biggest terrestrial predators, *Tyrannosaurus rex*. *Proc. R. Soc. B* **278**, 2682–2690. (doi:10.1098/rspb.2010.2497)

5. Krauss D, Robinson J. 2013 The biomechanics of a plausible hunting strategy for Tyrannosaurus rex. In *Tyrannosaurid paleobiology* (eds J Parrish, R Molnar, P Currie, E Koppelhus), pp. 251–264. Bloomington and Indianapolis, IN: Indiana University Press.
6. Bakker R. 1986 *Dinosaur heresies: new theories unlocking the mysteries of the dinosaurs and their extinction*. New York, NY: William Morrow and Co.
7. Paul GS. 1998 Limb design, function and running performance in ostrich-mimics and tyrannosaurs. *GAIA: Revista de Geociências* **15**, 257.
8. Paul GS. 2008 The extreme lifestyles and habits of the gigantic tyrannosaurid superpredators of the Late Cretaceous of North America and Asia. In Tyrannosaurus rex*: the tyrant king* (eds L Peter, C Kenneth), pp. 307–353. Bloomington, IN: Indiana University Press.
9. Schaller GB. 2009 *The Serengeti lion: a study of predator-prey relations*. Chicago, IL: University of Chicago Press.
10. Hutchinson JR, Bates KT, Molnar J, Allen V, Makovicky PJ. 2011 A computational analysis of limb and body dimensions in *Tyrannosaurus rex* with implications for locomotion, ontogeny, and growth. *PLoS ONE* **6**, e26037. (doi:10.1371/journal.pone.0026037)
11. Persons WS, Currie PJ. 2011 The tail of *Tyrannosaurus*: reassessing the size and locomotive importance of the *M. caudofemoralis* in non-avian theropods. *Anat. Rec.* **294**, 119–131. (doi:10.1002/ar.21290)
12. DeMaster DP, Stirling I. 1981 *Ursus maritimus*. *Mamm. Species* **Issue 145**, 1–7. (doi:10.2307/3503828)
13. Snively E *et al*. 2019 Lower rotational inertia and larger leg muscles indicate more rapid turns in tyrannosaurids than in other large theropods. *PeerJ* **7**, e6432. (doi:10.7717/peerj.6432)
14. Dempsey M, Cross SRR, Maidment SCR, Hutchinson JR, Bates KT. 2025 New perspectives on body size and shape evolution in dinosaurs. *Biol. Rev.* **100**, 1829–1860. (doi:10.1111/brv.70026)
15. Hutchinson JR. 2021 The evolutionary biomechanics of locomotor function in giant land animals. *J. Exp. Biol.* **224**, jeb217463. (doi:10.1242/jeb.217463)
16. Happ J. 2008 An analysis of predator-prey behavior in a head-to-head encounter between Tyrannosaurus rex and Triceratops. In *Tyrannosaurus rex the tyrant king* (eds P Larson, K Carpenter), pp. 355–370. Bloomington and Indianapolis, IN: Indiana University Press.
17. Alexander R. 1976 Estimates of speeds of dinosaurs. *Nature* **261**, 129–130. (doi:10.1038/261129a0)
18. Thulborn T. 1990 *Dinosaur tracks*. New York, NY: Springer.
19. Ruiz J, Torices A. 2013 Humans running at stadiums and beaches and the accuracy of speed estimations from fossil trackways. *Ichnos* **20**, 31–35. (doi:10.1080/10420940.2012.759115)
20. Hutchinson JR, Garcia M. 2002 *Tyrannosaurus* was not a fast runner. *Nature* **415**, 1018–1021. (doi:10.1038/4151018a)
21. Usami Y, Kinugasa R. 2017 A possibility of fast running of *Tyrannosaurus*. *DEStech Trans. Eng. Technol. Res.* **2017**, 118–126. (doi:10.12783/dtetr/amma2017/13347)
22. Coombs WP. 1978 Theoretical aspects of cursorial adaptations in dinosaurs. *Q. Rev. Biol.* **53**, 393–418. (doi:10.1086/410790)
23. Holtz TR. 1995 The arctometatarsalian pes, an unusual structure of the metatarsus of Cretaceous Theropoda (Dinosauria: Saurischia). *J. Vertebr. Paleontol*. **14**, 480–519. (doi:10.1080/02724634.1995.10011574)
24. Snively E, Russell AP. 2003 Kinematic model of tyrannosaurid (Dinosauria: Theropoda) arctometatarsus function. *J. Morphol*. **255**, 215–227. (doi:10.1002/jmor.10059)
25. Snively E, Russell AP, Powell GL. 2004 Evolutionary morphology of the coelurosaurian arctometatarsus: descriptive, morphometric and phylogenetic approaches. *Zool. J. Linn. Soc*. **142**, 525–553. (doi:10.1111/j.1096-3642.2004.00137.x)
26. Surring L, Burns M, Snively E, Barta D, Holtz T, Russell A, Witmer L, Currie P. 2022 Consilient evidence affirms expansive stabilizing ligaments in the tyrannosaurid foot. *Vertebr. Anat. Morphol. Palaeontol.* **10**, 49–64. (doi:10.18435/vamp29387)
27. Manning PL. 2008 *T. rex* speed trap. In *100 years of* Tyrannosaurus rex*: a symposium* (eds PL Larson, K Carpeneter), pp. 204–231. Bloomington and Indianapolis, IN: Indiana University Press.
28. Falkingham PL, Gatesy SM. 2014 The birth of a dinosaur footprint: subsurface 3D motion reconstruction and discrete element simulation reveal track ontogeny. *Proc. Natl Acad. Sci. USA* **111**, 18279–18284. (doi:10.1073/pnas.1416252111)
29. Avanzini M, Piñuela L, García-Ramos JC. 2012 Late Jurassic footprints reveal walking kinematics of theropod dinosaurs. *Lethaia* **45**, 238–252. (doi:10.1111/j.1502-3931.2011.00276.x)
30. Falkingham PL, Turner ML, Gatesy SM. 2020 Constructing and testing hypotheses of dinosaur foot motions from fossil tracks using digitization and simulation. *Palaeontology* **63**, 865–880. (doi:10.1111/pala.12502)
31. Lockley MG, Hunt AP. 1994 A track of the giant theropod dinosaur *Tyrannosaurus* from close to the Cretaceous/Tertiary boundary, northern New Mexico. *Ichnos* **3**, 213–218. (doi:10.1080/10420949409386390)
32. Manning PL, Ott C, Falkingham PL. 2008 A probable tyrannosaurid track from the hell creek formation (Upper Cretaceous), Montana, United States. *Palaios* **23**, 645–647. (doi:10.2110/palo.2008.p08-030r)
33. Zhang R, Han D, Ma S, Luo G, Ji Q, Xue S, Yang M, Li J. 2017 Plantar pressure distribution of ostrich during locomotion on loose sand and solid ground. *PeerJ* **5**, e3613. (doi:10.7717/peerj.3613)
34. Smith SD, Persons WS, Xing L. 2016 A tyrannosaur trackway at Glenrock, Lance Formation (Maastrichtian),Wyoming. *Cretaceous Res.* **61**, 1–4.
35. Caneer T, Molkestad T, Lucas SG. 2021 Tracks in the Upper Cretaceous of the Raton Basin possibly show tyrannosaurid rising from a prone position. *N. M. Mus. Nat. Hist. Sci. Bull.* **82**, 29–37.
36. McCrea RT, Buckley LG, Farlow JO, Lockley MG, Currie PJ, Matthews NA, Pemberton SG. 2014 A 'terror of tyrannosaurs': the first trackways of tyrannosaurids and evidence of gregariousness and pathology in Tyrannosauridae. *PLoS ONE* **9**, e103613. (doi:10.1371/journal.pone.0103613)
37. Gatesy SM, Biewener AA. 1991 Bipedal locomotion: effects of speed, size and limb posture in birds and humans. *J. Zool*. **224**, 127–147. (doi:10.1111/j.1469-7998.1991.tb04794.x)

38. Daley MA, Birn-Jeffery A. 2018 Scaling of avian bipedal locomotion reveals independent effects of body mass and leg posture on gait. *J. Exp. Biol.* **221**, jeb152538. (doi:10.1242/jeb.152538)
39. Gatesy SM. 1990 Caudofemoral musculature and the evolution of theropod locomotion. *Paleobiology* **16**, 170–186. (doi:10.1017/s0094837300009866)
40. Hartman S. 2013 *Stan*. See https://www.skeletaldrawing.com/theropods/tyrannosaurus-stan.
41. Hartman S. 2014 Tyrannosaurus-*Jane*. See https://www.skeletaldrawing.com/theropods/nanotyrannus-jane.
42. Hartman S. 2019 Tyrannosaurus rex *FMNH PR 2081 'Sue.'* See https://www.skeletaldrawing.com/theropods/tyrannosaurus-sue.
43. Hartman S. 2023 *Nation's* T. rex. See https://www.skeletaldrawing.com/theropods/nationstrex.
44. Bishop PJ, Hocknull SA, Clemente CJ, Hutchinson JR, Farke AA, Barrett RS, Lloyd DG. 2018 Cancellous bone and theropod dinosaur locomotion. Part III—inferring posture and locomotor biomechanics in extinct theropods, and its evolution on the line to birds. *PeerJ* **6**, e5777. (doi:10.7717/peerj.5777)
45. Alexander RM, Langman VA, Jayes AS. 1977 Fast locomotion of some African ungulates. *J. Zool.* **183**, 291–300. (doi:10.1111/j.1469-7998.1977.tb04188.x)
46. Alexander RMN. 1989 Mechanics of fossil vertebrates. *J. Geol. Soc. Lond.* **146**, 41–52. (doi:10.1144/gsjgs.146.1.0041)
47. Bates KT, Manning PL, Hodgetts D, Sellers WI. 2009 Estimating mass properties of dinosaurs using laser imaging and 3D computer modelling. *PLoS ONE* **4**, e4532. (doi:10.1371/journal.pone.0004532)
48. Carr TD. 2020 A high-resolution growth series of *Tyrannosaurus rex* obtained from multiple lines of evidence. *PeerJ* **8**, e9192. (doi:10.7717/peerj.9192)
49. Holtz TR. 2021 Theropod guild structure and the tyrannosaurid niche assimilation hypothesis: implications for predatory dinosaur macroecology and ontogeny in later Late Cretaceous Asiamerica. *Can. J. Earth Sci*. **58**, 778–795. (doi:10.1139/cjes-2020-0174)
50. Therrien F, Zelenitsky DK, Tanaka K, Voris JT, Erickson GM, Currie PJ, DeBuhr CL, Kobayashi Y. 2023 Exceptionally preserved stomach contents of a young tyrannosaurid reveal an ontogenetic dietary shift in an iconic extinct predator. *Sci. Adv*. **9**, eadi0505. (doi:10.1126/sciadv.adi0505)
51. Woodward HN, Tremaine K, Williams SA, Zanno LE, Horner JR, Myhrvold N. 2020 Growing up *Tyrannosaurus rex*: osteohistology refutes the pygmy '*Nanotyrannus*' and supports ontogenetic niche partitioning in juvenile *Tyrannosaurus*. *Sci. Adv.* **6**, eaax6250. (doi:10.1126/sciadv.aax6250)
52. Currie PJ. 2003 Allometric growth in tyrannosaurids (Dinosauria: Theropoda) from the Upper Cretaceous of North America and Asia. *Can. J. Earth Sci.* **40**, 651–665. (doi:10.1139/e02-083)
53. Bakker RT, Williams M. 1988 *Nanotyrannus*, a new genus of pygmy tyrannosaur, from the latest Cretaceous of Montana. *Hunteria* **1**, 1.
54. Persons WS, Currie PJ. 2016 An approach to scoring cursorial limb proportions in carnivorous dinosaurs and an attempt to account for allometry. *Sci. Rep*. **6**, 19828. (doi:10.1038/srep19828)
55. Longrich NR, Saitta ET. 2024 Taxonomic status of *Nanotyrannus lancensis* (Dinosauria: Tyrannosauroidea)—a distinct taxon of small-bodied tyrannosaur. *Foss. Stud.* **2**, 1–65. (doi:10.3390/fossils2010001)
56. Zanno LE, Napoli JG. 2025 *Nanotyrannus* and *Tyrannosaurus* coexisted at the close of the Cretaceous. *Nature* **648**, 357–367. (doi:10.1038/s41586-025-09801-6)
57. Greshko M. 2022 *Stan the* T. rex *found! World's most expensive fossil finds home in a new museum*. National Geographic. See https://www.nationalgeographic.com/science/article/stan-the-t-rex-found-worlds-most-expensive-fossil-finds-home-in-a-new-museum.
58. Sellers WI, Pond SB, Brassey CA, Manning PL, Bates KT. 2017 Investigating the running abilities of *Tyrannosaurus rex* using stress-constrained multibody dynamic analysis. *PeerJ* **5**, e3420. (doi:10.7717/peerj.3420)
59. Alexander RM, Maloiy GMO, Njau R, Jayes AS. 1979 Mechanics of running of the ostrich (*Struthio camelus*). *J. Zool*. **187**, 169–178. (doi:10.1111/j.1469-7998.1979.tb03941.x)
60. Carlson KJ, Jashashvili T, Houghton K, Westaway MC, Patel BA. 2013 Joint loads in marsupial ankles reflect habitual bipedalism versus quadrupedalism. *PLoS ONE* **8**, e58811. (doi:10.1371/journal.pone.0058811)
61. Cavanagh PR, Kram R. 1989 Stride length in distance running: velocity, body dimensions, and added mass effects. *Med. Sci. Sports Exerc*. **21**, 467–479.
62. Gatesy SM, Bäker M, Hutchinson JR. 2009 Constraint-based exclusion of limb poses for reconstructing theropod dinosaur locomotion. *J. Vertebr. Paleontol*. **29**, 535–544. (doi:10.1671/039.029.0213)
63. Currie PJ, Padian K (eds). 1997 *Encyclopedia of dinosaurs*. Amsterdam, The Netherlands: Elsevier.
64. Rothschild B, Tanke DH, Ford T. 2001 Theropod stress fractures and tendon avulsions as a clue to activity. In *Mesozoic vertebrate life* (eds DH Tanke, K Carpenter), pp. 331–336. Bloomington, IN: University of Inidiana Press.
65. Rolian C, Lieberman DE, Hamill J, Scott JW, Werbel W. 2009 Walking, running and the evolution of short toes in humans. *J. Exp. Biol.* **212**, 713–721. (doi:10.1242/jeb.019885)
66. Pizzuto F, Rago V, Bailey R, Tafuri D, Raiola G. 2016 The importance of foot strike patterns in running: a literature review. *Sport Sci*. **9**, 87–96.
67. Thulborn RA, Wade M. 1984 Dinosaur trackways in the Winton Formation (mid-Cretaceous) of Queensland. *Memoirs of the Queensland Museum, Nature* **21**, 413–517.
68. Hirt MR, Jetz W, Rall BC, Brose U. 2017 A general scaling law reveals why the largest animals are not the fastest. *Nat. Ecol. Evol*. **1**, 1116–1122. (doi:10.1038/s41559-017-0241-4)
69. Marmol-Guijarro A, Nudds R, Folkow L, Codd J. 2020 Examining the accuracy of trackways for predicting gait selection and speed of locomotion. *Front. Zool*. **17**, 17. (doi:10.1186/s12983-020-00363-z)

70. Heglund NC, Taylor CR. 1988 Speed, stride frequency and energy cost per stride: how do they change with body size and gait? *J. Exp. Biol.* **138**, 301–318. (doi:10.1242/jeb.138.1.301)
71. Sellers WI, Manning PL. 2007 Estimating dinosaur maximum running speeds using evolutionary robotics. *Proc. R. Soc. B* **274**, 2711–2716. (doi:10.1098/rspb.2007.0846)
72. Vogel S. 2025 *Life's devices: the physical world of animals and plants*. Princeton, NJ: Princeton University Press. (doi:10.2307/jj.25197188)
73. Osborn HF. 1917 Skeletal adaptations of *Ornitholestes, Struthiomimus, Tyrannosaurus*. *Bull. Am. Mus. Nat. Hist*. **35**, 733.
74. Hutchinson JR. 2004 Biomechanical modeling and sensitivity analysis of bipedal running ability. II. Extinct taxa. *J. Morphol*. **262**, 441–461. (doi:10.1002/jmor.10240)
75. Hutchinson JR, Anderson FC, Blemker SS, Delp SL. 2005 Analysis of hindlimb muscle moment arms in *Tyrannosaurus rex* using a three-dimensional musculoskeletal computer model: implications for stance, gait, and speed. *Paleobiology* **31**, 676–701. (doi:10.1666/0094-8373(2005)031[0676:AOHMMA]2.0.CO;2)
76. Christiansen P. 1998 Strength indicator values of theropod long bones, with comments on limb proportions and cursorial potential. *Gaia* **15**, 241–255.
77. Farlow JO, Smith MB, Robinson JM. 1995 Body mass, bone 'strength indicator,' and cursorial potential of *Tyrannosaurus rex*. *J. Vertebr. Paleontol.* **15**, 713–725. (doi:10.1080/02724634.1995.10011257)
78. Schroeder K, Lyons SK, Smith FA. 2021 The influence of juvenile dinosaurs on community structure and diversity. *Science* **371**, 941–944. (doi:10.1126/science.abd9220)
79. van Bijlert PA, van Soest AK, Schulp AS, Bates KT. 2024 Muscle-controlled physics simulations of bird locomotion resolve the grounded running paradox. *Sci. Adv.* **10**, eado0936. (doi:10.1126/sciadv.ado0936)
80. van Bijlert PA, Bates KT, Soest AK, Schulp A. 2023 Musculoskeletal constraints on top speed of Tyrannosaurus rex explored using 3D physics simulations (eds D Ehret, E Fulwood). In *Society of Vertebrate Paleontology, 83rd annual meeting*, p. 430. McLean, VA: Society of Vertebrate Paleontology.
81. Holliday CM, Ridgely RC, Sedlmayr JC, Witmer LM. 2010 Cartilaginous epiphyses in extant archosaurs and their implications for reconstructing limb function in dinosaurs. *PLoS ONE* **5**, e13120. (doi:10.1371/journal.pone.0013120)
82. Tsai HP, Middleton KM, Hutchinson JR, Holliday CM. 2018 Hip joint articular soft tissues of non-dinosaurian Dinosauromorpha and early Dinosauria: evolutionary and biomechanical implications for Saurischia. *J. Vertebr. Paleontol*. **38**, e1427593. (doi:10.1080/02724634.2017.1427593)
83. Tsai HP, Middleton KM, Hutchinson JR, Holliday CM. 2020 More than one way to be a giant: convergence and disparity in the hip joints of saurischian dinosaurs. *Evolution* **74**, 1654–1681. (doi:10.1111/evo.14017)
84. Bishop PJ, Falisse A, De Groote F, Hutchinson JR. 2021 Predictive simulations of running gait reveal a critical dynamic role for the tail in bipedal dinosaur locomotion. *Sci. Adv.* **7**, eabi7348. (doi:10.1126/sciadv.abi7348)
85. Manafzadeh AR, Gatesy SM, Nyakatura JA, Bhullar BAS. 2024 Fibular reduction and the evolution of theropod locomotion. *Nature* **637**, 113–117. (doi:10.1038/s41586-024-08251-w)
86. van Bijlert PA, van Soest AK, Schulp AS. 2021 Natural frequency method: estimating the preferred walking speed of *Tyrannosaurus rex* based on tail natural frequency. *R. Soc. Open Sci.* **8**, 201441. (doi:10.1098/rsos.201441)
87. Carrier DR, Walter RM, Lee DV. 2001 Influence of rotational inertia on turning performance of theropod dinosaurs: clues from humans with increased rotational inertia. *J. Exp. Biol.* **204**, 3917–3926. (doi:10.1242/jeb.204.22.3917)
88. Hutchinson JR. 2004 Biomechanical modeling and sensitivity analysis of bipedal running ability. I. Extant taxa. *J. Morphol*. **262**, 421–440. (doi:10.1002/jmor.10241)
89. Bishop PJ *et al*. 2018 The influence of speed and size on avian terrestrial locomotor biomechanics: predicting locomotion in extinct theropod dinosaurs. *PLoS ONE* **13**, e0192172. (doi:10.1371/journal.pone.0192172)
90. Bates KT, Manning PL, Margetts L, Sellers WI. 2010 Sensitivity analysis in evolutionary robotic simulations of bipedal dinosaur running. *J. Vertebr. Paleontol*. **30**, 458–466. (doi:10.1080/02724630903409329)
91. Boeye AT, Atkins-Weltman K, King JL, Swann S. 2026 Supplementary material from: Evidence of Bird-Like Foot Function in Tyrannosaurus. Figshare. (doi:10.6084/m9.figshare.c.8262492)